

## Vacuum-ultraviolet emission from high-pressure krypton\*

H. A. Koehler, L. J. Ferderber, D. L. Redhead, and P. J. Ebert

*Lawrence Livermore Laboratory, University of California, Livermore, California 94550*

(Received 8 August 1974; revised manuscript received 12 May 1975)

Krypton gas was excited by high-current relativistic electron bursts, and spectral and temporal characteristics of the uv continuum peaked at 1460 Å were measured as functions of pressure. Gas pressure ranged from 0.14 to 68 atm. The spectral full width at half-maximum of  $90 \pm 6$  Å was virtually independent of pressure from 3.4 to 68 atm. Exponential time constants for the buildup and decay of the uv intensity obeyed a  $P^{-1.5}$  pressure dependence for  $P < 4$  atm. Three pressure-independent intensity decay constants of  $9 \pm 1.5$ ,  $32 \pm 6$ , and  $350 \pm 70$  nsec were obtained for  $P > 6$  atm. The efficiency for conversion of electron kinetic energy to uv energy was  $(4 \pm 1.6)\%$ .

### I. INTRODUCTION

Experimental evidence of lasing in high-pressure noble gases excited by high-current relativistic electron beams<sup>1-3</sup> has stimulated much of the current interest in the characteristics of the spontaneous uv emission from these gases. Such measurements for high-pressure Ar and Xe excited by relativistic electrons were previously reported.<sup>4</sup> No spontaneous emission measurements for Kr under excitation conditions where uv lasing is obtained<sup>2</sup> have been reported. An investigation of Kr that parallels our earlier work with Ar and Xe is the subject of this report. Preliminary results were given previously.<sup>5</sup>

### II. EXPERIMENT

The experimental apparatus and procedure for this experiment were previously described in detail.<sup>4</sup> For completeness, a brief description of these follows. The electron sources were a Febetron 705 and a Febetron 706. The peak current of the Febetron 705 is  $7 \times 10^3$  A at 2-MV peak potential. The full width at half-maximum (FWHM) is 50 nsec. The average electron excitation energy is 1.3 MeV. The Febetron 705 was used to obtain spectra, peak power and efficiency data. The peak current of the Febetron 706 is  $7 \times 10^3$  A at 0.6-MV peak potential. The pulse FWHM is 2.5 nsec (5 nsec at the base).<sup>6</sup> Upon entering the gas cell, the average electron energy was approximately 0.2 MeV. Time constants for the buildup and decay of the uv intensity and efficiency data were obtained with the Febetron 706.

The stainless-steel excitation cell was pressurized with He to 100 atm and did not leak. Electrons entered the cell through a stainless-steel foil 0.13 mm thick. The excited gas was viewed

perpendicular to the electron beam axis through 2-mm-thick LiF windows, each having uv transmittance of 0.74 at 1470 Å.

High-purity Kr was admitted to the evacuated excitation cell after passing through a molecular sieve cooled in a solid-CO<sub>2</sub>-freon bath. Impurity concentrations, measured with a gas chromatograph were: O<sub>2</sub>, 1 ppm; N<sub>2</sub>, 3 ppm; H<sub>2</sub>O, 1 ppm; Ar, <2 ppm; CH<sub>4</sub>, <0.2 ppm; H<sub>2</sub>, <1 ppm; Xe, <10 ppm. The temperature of the gas before excitation was 22 °C. After each electron burst the Kr was reclaimed in a liquid N<sub>2</sub> cooled vessel for impurity analysis. Impurity concentrations were unchanged.

Time-integrated spectra were recorded on Kodak 101-01 uv-sensitive film located at the focal plane of a 0.5-m Sava-Namayoka-type vacuum monochromator. A 1200-line/mm grating blazed at 1500 Å was used. Density of the exposed film was measured with a Joyce-Loebl scanning microdensitometer.

At each pressure the continuum output intensity as a function of time was measured with ITT F4115 planar photodiodes of known uv sensitivity. A pinhole placed in the line-of-sight between the gas cell and the photodiode limited the output current to 5 A, well within the linear operating region of the photodiode. Tektronix 519 and 581 oscilloscopes recorded the photodiode signals. For measuring the buildup and decay time constants, two type 519 oscilloscopes were used in series. One had high vertical sensitivity and a relatively slow horizontal sweep speed to measure long-term decay. The other had lower sensitivity and a fast horizontal sweep to record the uv buildup and fast initial decay. The photodiode output connector was directly inserted in the first oscilloscope. The unattenuated signal passed through the first oscilloscope and through appropriate attenuators to the second. This minimized signal distortion due to cable dispersion.

### III. EXPERIMENTAL RESULTS

#### A. Spectra

Time-integrated spectra of the 1460-Å continuum were obtained for pressures ranging from 3.4 to 68 atm. Figure 1(a) shows a spectrum taken at 7 atm. The emission peaked at 1460 Å and did not change with gas pressure. The spectral FWHM of  $90 \pm 6$  Å was virtually independent of pressure. This behavior is shown in Fig. 1(b). No other emission was observed with film between 1100 and 2000 Å. The absorption line at 1470 Å results from resonance absorption by Xe.

#### B. Time constants

Time constants for the buildup and decay of the 1460-Å continuum were determined for pressures ranging from 0.14 to 68 atm. Photodiode oscilloscope traces taken at 20 atm are shown in Fig. 2. At each pressure, the traces were spliced absolutely in both time and amplitude to obtain the composite intensity curve. Each curve was fit

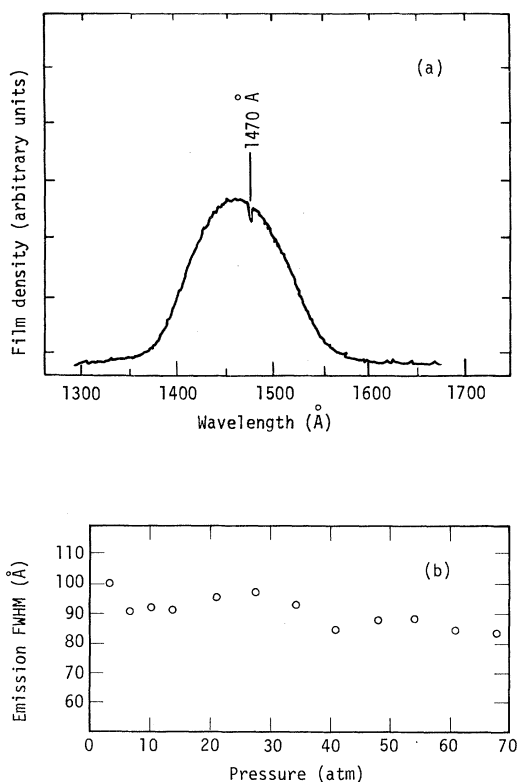


FIG. 1. (a) Time-integrated emission spectrum at 7 atm. (b) Pressure dependence of emission spectrum FWHM of Kr. Background was subtracted from photodensitometer recordings used in obtaining FWHM values. 1.3-MeV electrons excited the gas. Wavelength values are uncorrected for grating reflectivity and LiF transmittance.

with a sum of exponentials. A minimum of exponential terms was used to fit each curve to within the experimental error. All fits extended over a time of  $> 500$  nsec and over a dynamic voltage range of  $> 200$ .

Table I lists the time constants and the relative amplitudes at several gas pressures. Figure 3 is a plot of the time constants as a function of pressure.

Below 1 atm, one buildup and one decay term accurately fit each oscilloscope trace. Near 1 atm, it was necessary to introduce an additional decay term. The faster of the two decays had a  $P^{-1.5}$  pressure dependence. The slower decay was pressure independent, with a value near 350 nsec. At 6 atm, the buildup time constant could not be measured accurately because the buildup time was comparable to the duration of the excitation pulse and was obscured by a precursor pulse. At this pressure three decay components were needed to fit each trace. The slowest of these components had a 350-nsec time constant. The other two decay constants approached pressure-independent values of approximately 32 and 9 nsec. Above 10 atm, the amplitude ratio of the fast-decay components was approximately 3.5:1.

Similar to our observations in Ar and Xe,<sup>4</sup> a very fast precursor coinciding with the excitation pulse was also evident in Kr at low pressure. This precursor was not used in the curve fitting since it was of longer wavelength than the 1460-Å continuum. By using optical filters (Corning 0-54, 90-30, 3-138 and air), the wavelength of the precursor was determined to be  $2400 \pm 200$  Å. The amplitude of this emission increased linearly as the pressure was raised from 0.14 to 4 atm.

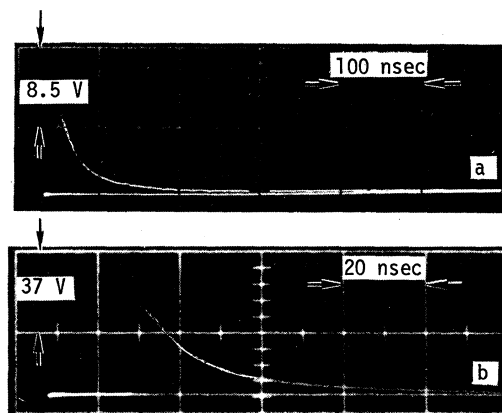


FIG. 2. Traces from (a) slow-sensitive and (b) fast-sensitive oscilloscopes showing photodiode output at  $P = 20$  atm. The gas was excited with a 2.5-nsec-FWHM electron burst. Baselines were obtained with zero-volt signal prior to gas excitation.

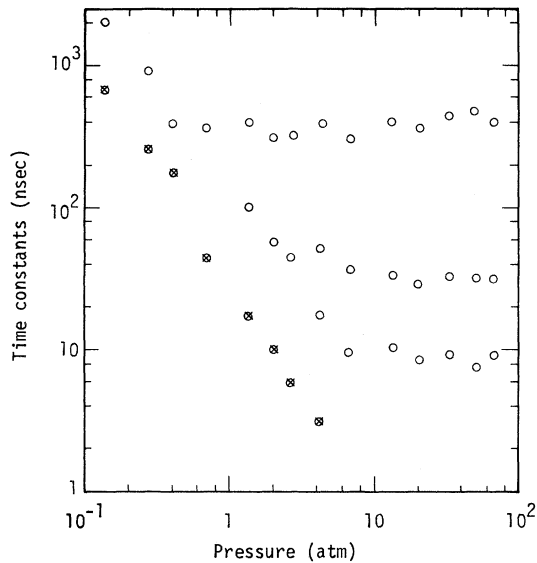


FIG. 3. Time constants for Kr buildup and decay as a function of pressure. Gas was excited with a 2.5-nsec-FWHM electron burst.

### C. Peak power and efficiency

Figure 4 shows the peak power emitted by approximately  $1.3 \text{ cm}^3$  of excited Kr as a function of pressure. The power values were calculated from the peak output voltage of the oscilloscope traces, knowing the detector geometry and sensitivity. Isotropic gas emission was assumed. Correction was made for LiF window transmission. No correction was made for uv transmission

through 4 cm of unexcited Kr gas. The peak power increased with pressure, reaching a maximum of  $3.1 \times 10^7 \text{ W}$  at 54 atm. At this pressure, the emission energy, obtained by measuring the area under the oscilloscope trace, was 1.5 J. To assure that no energy was lost in unobservable, long decay components, the photodiode output current was also integrated ( $RC = 35 \text{ } \mu\text{sec}$ ) and displayed on an oscilloscope. An identical result was obtained.

To obtain the efficiency for conversion of electron kinetic energy to uv energy, the electron energy absorbed per unit volume was calculated from the expression  $W_e = jF\gamma(dE/dx)\rho$ , where  $j$  is the electron current density ( $1700 \text{ A/cm}^2$ ),  $F$  is the geometrical transmission of the plate supporting the electron entrance window (0.6),  $\gamma$  is the FWHM of the electron burst (50 nsec),  $dE/dx$  is the effective collision energy-loss rate determined by a Monte Carlo calculation<sup>7</sup> ( $\sim 3.3 \text{ MeV/g cm}^{-2}$ ), and  $\rho$  is the gas density.<sup>8</sup> For these experimental conditions,  $W_e \cong 170\rho \text{ J/cm}^3$ . This approximation is valid if the variation in the energy-loss rate is small throughout the observed gas volume. On the basis of the Monte Carlo calculation, this is reasonable up to approximately 34 atm.

The uv energy density was divided by the electron-energy density at several gas pressures  $< 34 \text{ atm}$ . The efficiency was  $(4 \pm 1.6)\%$ .

### IV. ERROR

Sources of error in the emission spectra, the time constants and their corresponding amplitudes, and the output power and efficiency have been discussed in detail previously.<sup>4</sup> Table II lists the

TABLE I. Time constants and amplitudes for Kr buildup and decay obtained by fitting oscilloscope traces to  $[I(t) = \sum_i A_i e^{-t/\tau_i}]$ . Amplitudes were obtained with peak current density of  $500 \text{ A/cm}^2$  and an initial energy of approximately 0.2 MeV.

Pressure (atm)	Amplitude (arbitrary units)				Time constants (nsec)			
	$-A_1$	$A_2$	$A_3$	$A_4$	$\tau_1$	$\tau_2$	$\tau_3$	$\tau_4$
0.13	0.014			0.014	650			2000
0.27	0.074			0.074	260			900
0.54	0.71			0.71	175			390
0.68	1.2			1.2	45			360
1.3	4.7		2.7	1.3	17		100	400
2.0	30.0		10.0	1.7	10		57	310
2.7	34.0		16.0	2.2	6		45	330
4.4	32.0	21	17.0	1.8	3	17.0	52	390
6.8		42	42.0	2.7		9.5	37	300
13.0		140	50.0	2.5		10.5	34	400
20.0		150	70.0	2.5		8.5	29	370
34.0		200	47.0	2.1		9.5	33	440
52.0		180	33.0	1.3		7.5	32	480
68.0		90	14.0	0.47		9.0	32	400

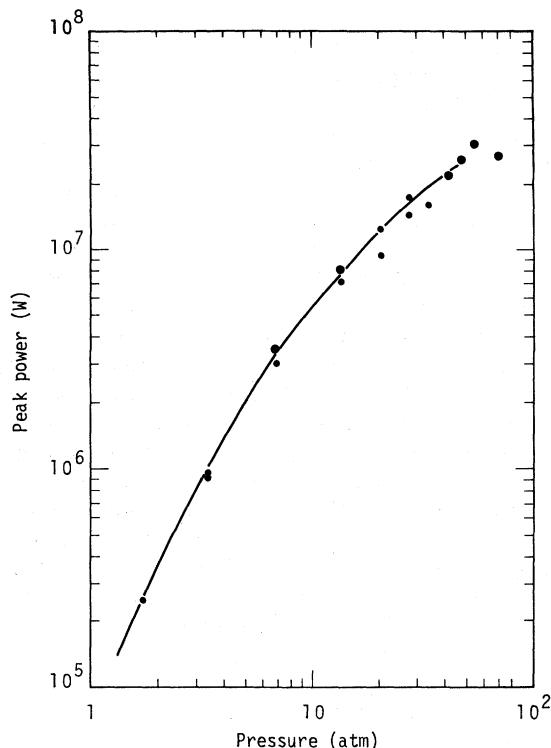


FIG. 4. Peak power of Kr emission from  $1.3 \text{ cm}^3$  of gas as a function of pressure. The points were corrected for transmittance of the LiF window, but not for unknown absorption by unexcited gas. 1.3-MeV electrons excited the gas.

random errors in this experiment.

In addition to the uncertainties in Table II, sources of systematic error were present. These were: grating reflectivity, uv-window transmittance, gas impurities, excitation power level, and self-absorption by unexcited gas.

The reflectivity of the grating used in these experiments was not measured; therefore, no correction was made. The reflectivity of a similar blaze-angle grating varied from 20% to 23% across the Kr emission continuum.<sup>9</sup> The correction of this kind of variation on  $\lambda_{\text{max}}$  and on the spectral FWHM is negligible. A negligible correction is also obtained for the wavelength variation of the LiF transmittance.

No systematic study of the effect of impurities on these results was made. However, some data were obtained without the cooled molecular sieve in the gas-fill system. The  $\text{H}_2\text{O}$  and Xe impurity concentrations for these measurements were 10 ppm and 50 ppm, respectively. Identical oscilloscope traces were obtained with and without the molecular sieve. The Xe absorption line in the continuum was the only obvious evidence of an impurity.

To determine if the time constants were influenced by the high excitation current, some data were obtained with less than one-tenth the usual current density. The relative amplitude of the 350-nsec decay component increased with decreasing current. The time constants and other

TABLE II. Summary of random experimental errors.

Error sources		Estimated error
Emission peak	$\pm 0.5 \text{ mm}$	$\pm 8.5 \text{ \AA}$
Half-intensity location (FWHM)	$\pm 0.15 \text{ mm}$	$\pm 6 \text{ \AA}$
Decay and buildup time constants		$\pm 20\%$
Oscilloscope trace reading		
(0.5) trace width	$\pm 0.2 \text{ mm}$	
Amplitude of decay components		$\pm 50\%$ (9 nsec)
		$\pm 25\%$ (32 nsec)
		$\pm 20\%$ (350 nsec)
Decay time constants	$\pm 20\%$	
Breakout of uv emission pulse	$\pm 0.3 \text{ nsec}$	
Amplitude of buildup component		$\pm 25\%$
uv output energy		$\pm 22\%$
Photodiode sensitivity	$\pm 20\%$	
Oscilloscope attenuators	$\pm 5\%$	
Oscilloscope dc-calibration	$\pm 2\%$	
Oscilloscope trace reading	$\pm 3\%$	
Optical geometry factor	$\pm 6\%$	
LiF window transmission	$\pm 5\%$	
Conversion efficiency		$\pm 41\%$
uv output energy	$\pm 22\%$	
Excited gas volume	$\pm 20\%$	
Electron current density	$\pm 20\%$	
$dE/dx$	$\pm 20\%$	

relative amplitudes were unchanged.

No corrections were made for self-absorption by unexcited gas.

## V. DISCUSSION

The behavior of Kr under intense electron excitation is very similar to that of Ar and Xe. Potential curves for Ar<sup>10</sup> and Xe,<sup>11</sup> together with kinetic models<sup>10,12</sup> for the formation and decay of excited molecules, serve as guides to discuss qualitatively some of our observations.

### A. Spectra

Nearly all of the radiant energy emitted was in the uv continuum peaked at 1460 Å. This is very close to the 1457-Å wavelength at which oscillation occurs,<sup>2</sup> but is in marked disagreement with 1440 Å obtained for proton excitation<sup>13</sup> and 1425 Å obtained for low-intensity electron excitation.<sup>14</sup> These differences could be the consequence of different grating reflectivities. The continuum is attributed to radiative transitions from the  $^1\Sigma_u^+$  and  $^3\Sigma_u^+$  states to the  $^1\Sigma_g^+$  molecular ground state. These transitions are spectrally unresolvable. No emission was detected at shorter wavelengths. This indicates resonance trapping of photons from atomic transitions and the absence of photons from radiative decay of higher-energy molecular states to the molecular ground state. A spectral FWHM of  $90 \pm 6$  Å is consistent with spectral widths reported by Leichner and Ericson<sup>14</sup> and Stewart *et al.*<sup>13</sup> Weak emission observed at  $2400 \pm 200$  Å was associated with the very fast precursor and may be evidence of radiative recombination of electrons with atomic ions.<sup>15</sup> The lack of strong, longer wavelength uv indicates rapid collisional deexcitation of the large initial atomic and molecular ion population to lower excited atomic states. Infrared radiation arising from molecular transitions to the  $^1\Sigma_u^+$  and  $^3\Sigma_u^+$  states was suggested by Mulliken<sup>11</sup> and was observed in Ar by Arai and Firestone.<sup>16</sup> Our experiments did not cover this spectral region.

### B. Time constants

Time constants at low pressure ( $P < 4$  atm) have a  $P^{-1.5}$  pressure dependence that is evidently as-

sociated with the formation of radiative molecules. Above 6 atm, excellent fits to the oscilloscope traces were obtained with three pressure-independent, exponential decay constants. These results, together with spectral data, suggest that two spectrally unresolvable molecular states ( $^1\Sigma_u^+$ ,  $^3\Sigma_u^+$ ) decay independently to the molecular ground state ( $^1\Sigma_g^+$ ). Since singlet-singlet transitions are more probable than triplet-singlet transitions, it is reasonable to assign the 9-nsec decay to the  $^1\Sigma_u^+$  state and the 32-nsec decay to the  $^3\Sigma_u^+$  state. The 350-nsec decay could result from undetected infrared transitions from higher excited molecular levels to the  $^1\Sigma_u^+$  and  $^3\Sigma_u^+$  molecular states.<sup>11</sup> The ratio of the amplitudes of the 9- and 32-nsec decay components was approximately 3.5 to 1. This implies that the initial concentrations of the singlet and triplet radiative molecules were approximately equal.

The  $P^{-1.5}$  pressure dependence of the time constants obtained here for  $P < 4$  atm agrees with that reported by Bouciqué and Mortier<sup>17</sup> and by Leichner and Ericson<sup>14</sup> for Kr at  $P < 1$  atm. The pressure-dependent buildup time constant and the 350-nsec pressure-independent decay constant are in excellent agreement with those reported by Leichner and Ericson. The longer decay constant observed by Bouciqué and Mortier (1.7  $\mu$ sec) was not found. Our results indicated that the excitation current density affected only the relative amplitude of the 350-nsec time constant. An even longer decay component might have been effectively suppressed because of the high excitation levels used in these experiments.

### C. Output power and efficiency

The maximum power density observed for the Kr continuum under 1.3-MeV electron excitation was  $2.4 \times 10^7$  W/cm<sup>3</sup> at 54 atm. The efficiency of approximately  $(4 \pm 1.6)\%$  does not agree with the value of 12% reported by Stewart *et al.*<sup>13</sup>

## ACKNOWLEDGMENTS

The authors thank D. Jones, G. Clough, S. Stribling, and V. Gregory for the help in the mechanical aspects of these experiments.

\*Work performed under the auspices of the USERDA.

<sup>1</sup>H. A. Koehler, L. J. Ferderber, D. L. Redhead, and P. J. Ebert, Appl. Phys. Lett. **21**, 198 (1972).

<sup>2</sup>P. W. Hoff, J. C. Swingle, and C. K. Rhodes, Appl.

Phys. Lett. **23**, 245 (1973).

<sup>3</sup>W. M. Hughes, J. Shammon, and R. Hunter, Appl. Phys. Lett. **24**, 488 (1974).

<sup>4</sup>H. A. Koehler, L. J. Ferderber, D. L. Redhead, and

- P. J. Ebert, *Phys. Rev. A* **9**, 768 (1974).
- <sup>5</sup>H. A. Koehler, L. J. Ferderber, and P. J. Ebert, *Bull. Am. Phys. Soc.* **19**, 157 (1974).
- <sup>6</sup>A different electron tube was used in these experiments. The excitation pulse width depends on tube characteristics. A 1.6-nsec-FWHM pulse was measured with the tube used in Ref. 4.
- <sup>7</sup>M. J. Berger and S. M. Seltzer, NASA Report No. SP-169, 1968 (unpublished). Calculations were carried out with program ETRAN-15.
- <sup>8</sup>G. A. Cook, *Argon, Helium and the Rare Gases* (Interscience, New York, 1961), p. 268. The Ottawa virial coefficients were used.
- <sup>9</sup>G. S. Hurst, T. E. Bortner, and T. D. Strickler, *Phys. Rev.* **178**, 4 (1969).
- <sup>10</sup>D. C. Lorents and R. E. Olson, Stanford Research Institute Semi-Annual Technical Report No. 1, 1972 (unpublished).
- <sup>11</sup>R. S. Mulliken, *J. Chem. Phys.* **52**, 5170 (1970).
- <sup>12</sup>C. W. Werner, E. V. George, P. W. Hoff, and C. K. Rhodes, *Appl. Phys. Lett.* **25**, 235 (1974).
- <sup>13</sup>T. E. Stewart, G. S. Hurst, T. E. Bortner, J. E. Parks, F. W. Martin, and H. L. Weidner, *J. Opt. Soc. Am.* **60**, 1290 (1970).
- <sup>14</sup>P. K. Leichner and R. J. Ericson, *Phys. Rev. A* **9**, 251 (1974).
- <sup>15</sup>J. A. Viecelli, LLL Report No. UCRL-51374, 1973 (unpublished).
- <sup>16</sup>S. Arai and R. F. Firestone, *J. Chem. Phys.* **50**, 4575 (1969).
- <sup>17</sup>R. Bouciqué and P. Mortier, *J. Phys. D* **3**, 1905 (1970).

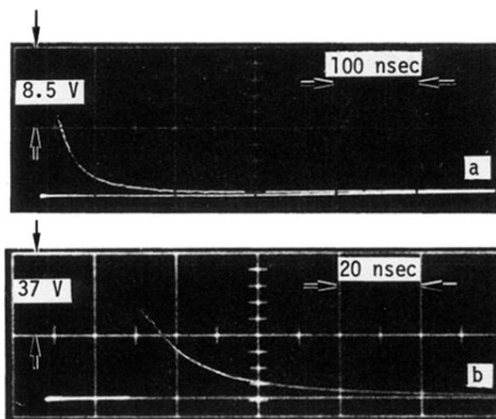


FIG. 2. Traces from (a) slow-sensitive and (b) fast-insensitive oscilloscopes showing photodiode output at  $P = 20$  atm. The gas was excited with a 2.5-nsec-FWHM electron burst. Baselines were obtained with zero-volt signal prior to gas excitation.